Title

Simultaneous PET/MRI Imaging During Mouse Cerebral Hypoxia-ischemia.

Journal

Journal of Visualized Experiments, 2015(103)

ISSN

1940-087X

Authors

Ouyang, Yu
Judenhofer, Martin S
Walton, Jeffrey H
et al.

Publication Date

2015

DOI

10.3791/52728

Peer reviewed

Video Article

Simultaneous PET/MRI Imaging During Mouse Cerebral Hypoxia-ischemia

Yu Ouyang[1], Martin S. Judenhofer[1], Jeffrey H. Walton[1,2], Jan Marik[3], Simon P. Williams[3], Simon R. Cherry[1,4]

[1]Department of Biomedical Engineering, University of California, Davis

[2]Nuclear Magnetic Resonance Facility, University of California, Davis

[3]Biomedical Imaging, Genentech, Inc

[4]Department of Radiology, University of California, Davis

Correspondence to: Yu Ouyang at youyang@ucdavis.edu

URL: http://www.jove.com/video/52728
DOI: doi:10.3791/52728

Keywords: Medicine, Issue 103, Stroke, Hypoxia-Ischemia, Brain, Positron Emission Tomography, Magnetic Resonance Imaging (MRI), Neuroimaging, cerebral hypoxia-ischemia, simultaneous imaging

Date Published: 9/20/2015

Citation: Ouyang, Y., Judenhofer, M.S., Walton, J.H., Marik, J., Williams, S.P., Cherry, S.R. Simultaneous PET/MRI Imaging During Mouse Cerebral Hypoxia-ischemia. *J. Vis. Exp.* (103), e52728, doi:10.3791/52728 (2015).

Abstract

Dynamic changes in tissue water diffusion and glucose metabolism occur during and after hypoxia in cerebral hypoxia-ischemia reflecting a bioenergetics disturbance in affected cells. Diffusion weighted magnetic resonance imaging (MRI) identifies regions that are damaged, potentially irreversibly, by hypoxia-ischemia. Alterations in glucose utilization in the affected tissue may be detectable by positron emission tomography (PET) imaging of 2-deoxy-2-(^{18}F)fluoro-D-glucose ([^{18}F]FDG) uptake. Due to the rapid and variable nature of injury in this animal model, acquisition of both modes of data must be performed simultaneously in order to meaningfully correlate PET and MRI data. In addition, inter-animal variability in the hypoxic-ischemic injury due to vascular differences limits the ability to analyze multi-modal data and observe changes to a group-wise approach if data is not acquired simultaneously in individual subjects. The method presented here allows one to acquire both diffusion-weighted MRI and [^{18}F]FDG uptake data in the same animal before, during, and after the hypoxic challenge in order to interrogate immediate physiological changes.

Video Link

The video component of this article can be found at http://www.jove.com/video/52728/

Introduction

Worldwide, stroke is the second leading cause of death and a major cause of disability [1]. The cascade of biochemical and physiological events that occur during and acutely following a stroke event occurs rapidly and with implications for tissue viability and ultimately outcome [2]. Cerebral hypoxia-ischemia (H-I), which leads to hypoxic-ischemic encephalopathy (HIE), is estimated to affect up to 0.3% and 4% of full-term and preterm births, respectively [3,4]. The mortality rate in infants with HIE is approximately 15% to 20%. In 25% of HIE survivors, permanent complications arise as a result of the injury, including mental retardation, motor deficits, cerebral palsy, and epilepsy [3,4]. Past therapeutic interventions have not proven worthy of adoption as standard of care, and consensus has yet to be reached that the most advanced methods, based on hypothermia, are effectively reducing morbidity [3,5]. Other issues of contention include method of administration of hypothermia and patient selection [6]. Thus, strategies for neuroprotection and neurorestoration are still a fertile area for research[7].

Rat models of cerebral H-I have been available since the 1960s, and subsequently were adapted to mice [8,9]. Due to the nature of the model and the location of the ligation, there is inherent variability in the outcome due to difference in collateral flow between animals [10]. As a result, these models tend to be more variable compared to similar models such as middle cerebral artery occlusion (MCAo). Real time measurement of physiological changes has been demonstrated with laser Doppler flowmetry as well as diffusion-weighted MRI [11]. The observed intra-animal variability in cerebral flow blood during and immediately after hypoxia, as well as in acute outcomes such as infarct volume and neurological deficit, suggest that simultaneous acquisition and correlation of multimodal data would be beneficial.

Recent advances in simultaneous positron emission tomography (PET) and magnetic resonance imaging (MRI) have allowed for new possibilities in preclinical imaging [12-14]. The potential advantages of these hybrid, combined systems for preclinical applications have been described in the literature [15,16]. While many preclinical questions can be addressed by imaging an individual animal sequentially or by imaging separate animal groups, certain situations – for example, when each instance of an event such as stroke manifests itself uniquely, with rapidly evolving pathophysiology – make it desirable and even necessary to use simultaneous measurement. Functional neuroimaging provides one such example, where simultaneous 2-deoxy-2-(^{18}F)fluoro-D-glucose ([^{18}F]FDG) PET and blood-oxygen-level dependent (BOLD) MRI has recently been demonstrated in rat whisker stimulation studies [14].

Here, we demonstrate simultaneous PET/MRI imaging during onset of a hypoxic-ischemic stroke in which brain physiology is not at steady state, but instead is rapidly and irreversibly changing during hypoxic challenge. Changes in water diffusion, as measured by MRI and quantified by the apparent diffusion coefficient (ADC) derived from diffusion-weighted imaging (DWI), has been well characterized for stroke in clinical and preclinical data [17,18]. In animal models such as MCAo, diffusion of water in affected brain tissue drops rapidly due to the bioenergetic cascade leading to cytotoxic edema [18]. These acute changes in ADC are also observed in rodent models of cerebral hypoxia-ischemia [11,19]. [^{18}F]FDG PET imaging has been used in stroke patients to assess changes in local glucose metabolism [20], and a small number of *in vivo* animal studies have also used [^{18}F]FDG [21], including in the cerebral hypoxia-ischemia model [22]. In general, these studies show decreased glucose utilization in ischemic regions, although a study using a model with reperfusion found no correlation of these metabolic changes with later infarction development [23]. This is in contrast to diffusion changes which have been associated with the irreversibly damaged core [21]. Thus, it is important to be able to obtain the complementary information derived from [^{18}F]FDG PET and DWI in a simultaneous manner during the evolution of stroke, as this is likely to yield meaningful information about the progression of injury and the impact of therapeutic interventions. The method we describe here is readily amenable to use with a variety of PET tracers and MRI sequences. For instance, [^{15}O]H_2O PET imaging along with DWI and perfusion-weighted images (PWI) from MRI may be used to further explore the development of the ischemic penumbra and validate current techniques within the stroke imaging field.

Protocol

All animal handling and procedures described herein, and according to the Animal Research: Reporting In Vivo Experiments (ARRIVE) guidelines, were performed in accordance with protocols approved by the Association for Assessment of Accreditation of Laboratory Animal Care (AAALAC) International accredited Institutional Animal Care and Use Committee at the University of California, Davis. Proper surgery should not result in signs of any pain or discomfort in the animal, but proper steps should be taken if these signs are observed, including administration of analgesics or in some cases, euthanasia. The right side of the animals was chosen arbitrarily for the unilateral procedure described.

1. Unilateral Common Carotid Artery (CCA) Ligation

1. Prepare sterile field with sterilized surgical tools and materials positioned conveniently. Ensure heating pad is warmed to 37 °C with temperature probe placed securely on the pad. Be sure to use a sterile drape to cover the surgical site.
2. Anesthetize animal (isoflurane, 1-3% in air at 0.5-1 L/min), and place animal in a supine position with the tail facing away. Check anesthetization by pinching the toe - this should elicit no reaction if the animal is properly anesthetized. Apply ophthalmic ointment to the eyes.
3. Apply depilation cream to lower neck to upper chest area using 1-2 cotton swabs. Wait 1-3 min, and then remove hair and cream using wet gauze or alcohol swabs. Swab incision area with Betadine in a circular manner from inside to outside, and then change into sterile surgical gloves.
4. Using surgical scissors, make an incision of around 1 cm along the midline of the lower neck. Carefully separate outer skin from surrounding fascia using surgical scissors.
5. Using two McPherson micro iris suturing forceps, separate the right common carotid artery from fascia, taking care to avoid damaging veins or disturbing the vagus nerve.
6. Using the forceps on the right, exteriorize the right CCA in a stable position. Apply several drops of saline to prevent drying. Pass a suitable length (2-3 cm) of 6-0 silk suture underneath the right CCA, and ligate using a double square knot. Optionally, ligate again using a second length of 6-0 silk suture.
7. Reposition right CCA and clean excess fluid from opening using a sterile sponge tipped swab. Close the incision with 6-0 silk suture. Apply lidocaine topically up to 7 mg/kg.
8. Allow the animal to recover from anesthesia until ambulatory (approximately 30 min) and perform post-surgical monitoring until animal is ready for imaging.

2. Preparation for Imaging: System and Hardware Checks

1. Set up hardware and software for the MRI and PET systems and check their functionality as follows. Ensure all physical connections are secure and software settings are appropriately selected.
    1. Ensure the PET system is at the prescribed operating temperature of 5 °C using the air cooling system.
    2. Mount PET system inside the MRI bore, aligning the PET and MRI field of view (FOV) centers using known axial offsets. Mount the MRI coil inside the bore of the PET system and center the coil with the PET system and MRI magnet centers.
    3. Turn on PET electronics for power and bias voltage (Note: steps will vary by instrument). Perform a quick (5 min) scan using a ^{68}Ge cylinder and check the resulting sinogram to ensure all detectors are operational.
    4. Optionally acquire data to be used for a PET/MRI transformation matrix for co-registration purposes: Fill a three-dimensional phantom (*e.g.*, three filled spheres) with 200 µCi of ^{18}F aqueous solution and acquire for 15 min with PET. Acquire anatomical MRI data: in the Scan Control Window, select the multi-slice multi-echo (MSME) sequence (see **Table 1**). Repeat for all three major orientations: axial, sagittal, and coronal.
2. Check the infusion pump settings and operation. Set the pump to 4.44 µl per minute, which in 45 min of constant infusion delivers a total volume of 200 µl, the typical recommended limit for i.v. injection in a 20 g animal.
3. Check the heater operation and confirm that the temperature output is sufficient to keep the animal warm (37 °C). Check that the temperature and respiratory monitoring is operational in preparation for animal placement on the animal bed.
4. Check the operation of the O_2 and N_2 flowmeters (for 0.5 L/min: O_2 at 57.2 mg/min and N_2 at 0.575 g/min) by powering on both with the compressed air source off and O_2 and N_2 sources on. To avoid the risk of damaging the flowmeters, do not turn them on without sufficient input pressure.
5. Ensure that isoflurane vaporizer is sufficiently filled. Prior to imaging, start isoflurane anesthesia flow at 1-2% and 0.5 to 1 L/min.

6. Prepare animal bed by ensuring that the anesthesia, respiratory pad, and heater systems are positioned securely and functional. For additional PET/MRI co-registration accuracy, fiducial markers (*e.g.*, capillary tubes filled with radiotracer at a similar concentration as injected for imaging) may be attached to the animal bed within the field of view.

3. Imaging workflow

After all necessary equipment checks are completed, proceed to imaging as follows:

1. Anesthetize the animal with isoflurane and insert tail vein catheter (28 G needle, PE-10 tubing less than 5 cm) filled with heparinized saline (0.5 ml heparin, 1,000 USP/ml, in 10 ml saline). Warming the animal and/or tail may improve catheter insertion accuracy. Optionally place a drop of cyanoacrylate adhesive on the site of insertion to secure the IV line.
2. Transfer the animal to the prepared animal bed. Ensure that the animal's head is secure, with upper incisors secured by the tooth bar and ear bars in place if being used.
3. Apply ophthalmic ointment to eyes to prevent drying. Insert rectal probe thermometer. Ensure that temperature and respiration readings are functional.
4. Draw the radiotracer dose (around 600 µCi in 200 µl) to be injected into heparinized PE-10 tubing of appropriate length – approximately 3 m for PE-10 tubing and a volume of 200 µl. Connect one end of this tubing to the infusion pump syringe, and the other to the tail vein catheter line, taking care not to create punctures in the tubing.
5. Slide the animal bed forward into the bore of the magnet, making sure not to disturb the positioning of the MRI coil and any lines or cables, especially the anesthesia tubing. Ensure that the center of the brain is aligned with the centers of the MRI coil, PET system, and MRI magnet.
6. Perform tuning and matching of the MRI coil by rotating the adjustment knobs on the coil, minimizing impedance (check coil specifications) and frequency (300 MHz for ^{1}H at 7 Tesla) mismatches by observing the display of the high power preamplifier.
7. (MRI) After tuning and matching, acquire a scout image: select a RARE tripilot sequence and run the sequence from the Scan Control Window. Check positioning of the animal, repeating steps 3.5 and 3.6 as necessary. Reset shims to zero value.
8. (MRI) Acquire a localized, point-resolved spectroscopic scan (PRESS) in a volume within the brain: Run a PRESS sequence (see **Table 1**) in a rectangular volume with dimensions 3.9 mm × 6 mm × 9 mm. Check water line width using the CalcLineWidth macro command. If the full width at half-maximum (FWHM) value is acceptable (*e.g.,* 0.2 ppm), continue to step 3.10. If not, proceed to step 3.9.
9. (MRI) Acquire a field map: Run a FieldMap sequence (see **Table 1**). Use the resulting data for a multi-angle projection shim (MAPSHIM) by running the MAPSHIM macro command and selecting linear and second order (z^2) local adjustments. Repeat step 3.8.
10. (MRI) Position the slice plan for the DWI scan (see **Table 1**): using the Geometry Editor, ensure that the acquisition FOV is positioned to acquire the desired volume of interest within the brain. If the resulting slice plan is aligned as desired, copy this slice plan in the Scan Control Window for all subsequent DWI scans. Begin acquisition.
11. (PET) With the PET acquisition prepared and ready to begin, start the infusion pump. After the pre-determined delay in which saline from the catheter has been injected, begin the PET acquisition (see **Table 1**) in order to capture the entry of radiotracer. Monitor the count rate and look for gradual increase in counts indicative of a successful injection.
12. After 10-15 min, initiate the hypoxic challenge concurrent with step 3.12. To initiate hypoxic challenge, turn off medical air flow and immediately power on O_2 and N_2 flowmeters with the predetermined settings to deliver 8% oxygen and 92% nitrogen, and reduce isoflurane to 0.8%. **Do not** power on flowmeters without input pressure.
13. (MRI) At the same time as step 3.12, begin DWI acquisition prepared in step 3.10 (scan "H1").
14. (MRI) Begin DWI acquisition (scan "H2"), prepared in step 3.10, immediately after scan H1 is completed. End hypoxic challenge by powering off flowmeters, restoring medical air flow, and returning isoflurane concentration to a suitable value based on physiological monitoring.
15. (MRI) Acquire a post-hypoxia DWI scan prepared in step 3.10. Turn off the infusion pump after this scan has completed.
16. (MRI) Acquire anatomical images in the axial and sagittal planes. In the Scan Control Window – select the MSME sequence (see **Table 1**). Using the Geometry Editor, ensure that the acquisition FOV covers the brain.
17. Remove animal, return to cage when ambulatory and monitor for signs of morbidity, euthanizing if necessary with administration of CO_2 followed by cervical dislocation as a secondary method.

Representative Results

Figure 1 demonstrates the result of a proper ligation of the common carotid artery, prior to closing the wound with 6-0 silk suture.

In this method, data obtained from imaging is highly dependent upon the temporal arrangement of the experiment, which in turn dictates and is also dictated by experimental limitations including image acquisition schemes and equipment setup. These and other considerations are further explored in the Discussion section. With the protocol described herein, the physical setup of the equipment (**Figure 2A**) allows for uninterrupted multi-modal image acquisition before, during, and after (**Figure 2B**) rapid introduction of the hypoxic challenge (**Figure 2C**).

In this animal model, as with many ischemic stroke models, changes in diffusion are detectable rapidly after insult (see **Figure 3A** for a representative example). As our method does not fundamentally alter the cerebral H-I model, diffusion changes can be reproduced in a robust manner – **Figure 3B** demonstrates the evolving percent differences in ADC_z (ADC in the z-direction) between the contralateral (non-occluded, left) and ipsilateral (occluded, right) sides of the brain, %L-R, (n = 6 for scan H2, n = 5 for all other time points). As expected, ADC values on the occluded side of the brain decrease as the injury progresses. **Figure 3C** shows an example coronal slice from the DWI sequence, as well as a sagittal slice demonstrating the limited axial extent of the FOV (8 mm) for the sequence used. Details regarding limitations imposed upon the echo planar imaging (EPI) sequence used for DWI are described in the Discussion section. In short, image quality obtained with the proposed imaging framework is dependent on system performance characteristics, and EPI-based DWI sequences in particular may expose suboptimal hardware conditions or acquisition parameters (see **Figure 5B**). That significant differences were observed between baseline and subsequent ADC %L-R values ($p < 0.05$, unpaired *t*-test) suggests that this is a robust parameter to interrogate using our experimental setup.

Concurrent with changes in ADC, hemispherical differences were observed in the uptake of [^{18}F]FDG after beginning the hypoxic challenge and during scan H2 (%11 mean L-R difference, n=3). In two of three cases, ipsilateral [^{18}F]FDG uptake decreased relative to contralateral uptake

after hypoxia (see **Figure 4** for a representative example), though this was not true in all cases likely due to animal variability. **Figure 5A** shows an example where the relative difference in [^{18}F]FDG uptake between the two hemispheres was not as expected in one animal (blue). **Figure 5A** also shows an example where, while [^{18}F]FDG uptake was as expected following hypoxia, the animal died at the end of scan H2.

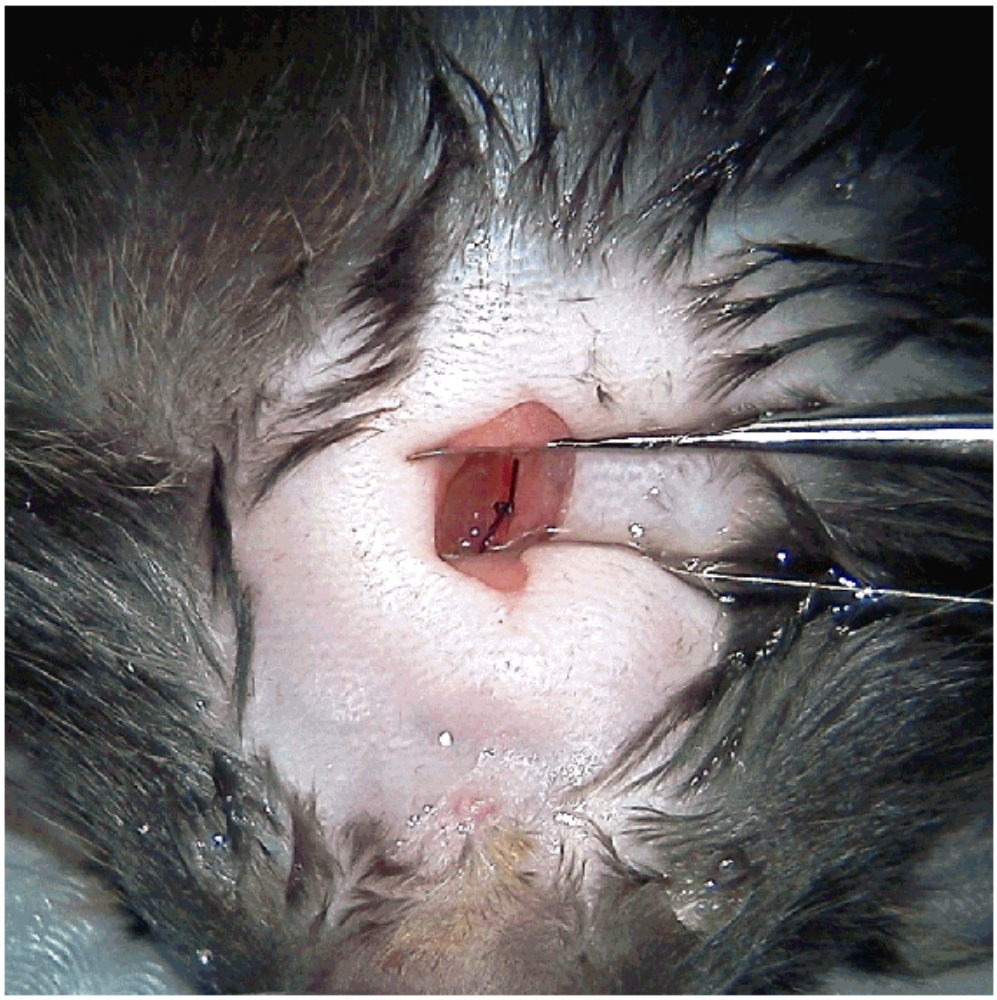

Figure 1. Example of the right common carotid artery ligated with 6-0 silk suture. The animal is supine with its head pointed towards the bottom of the image. The area around the incision has been depilated, and the incision is being held open with forceps for visualization. Please click here to view a larger version of this figure.

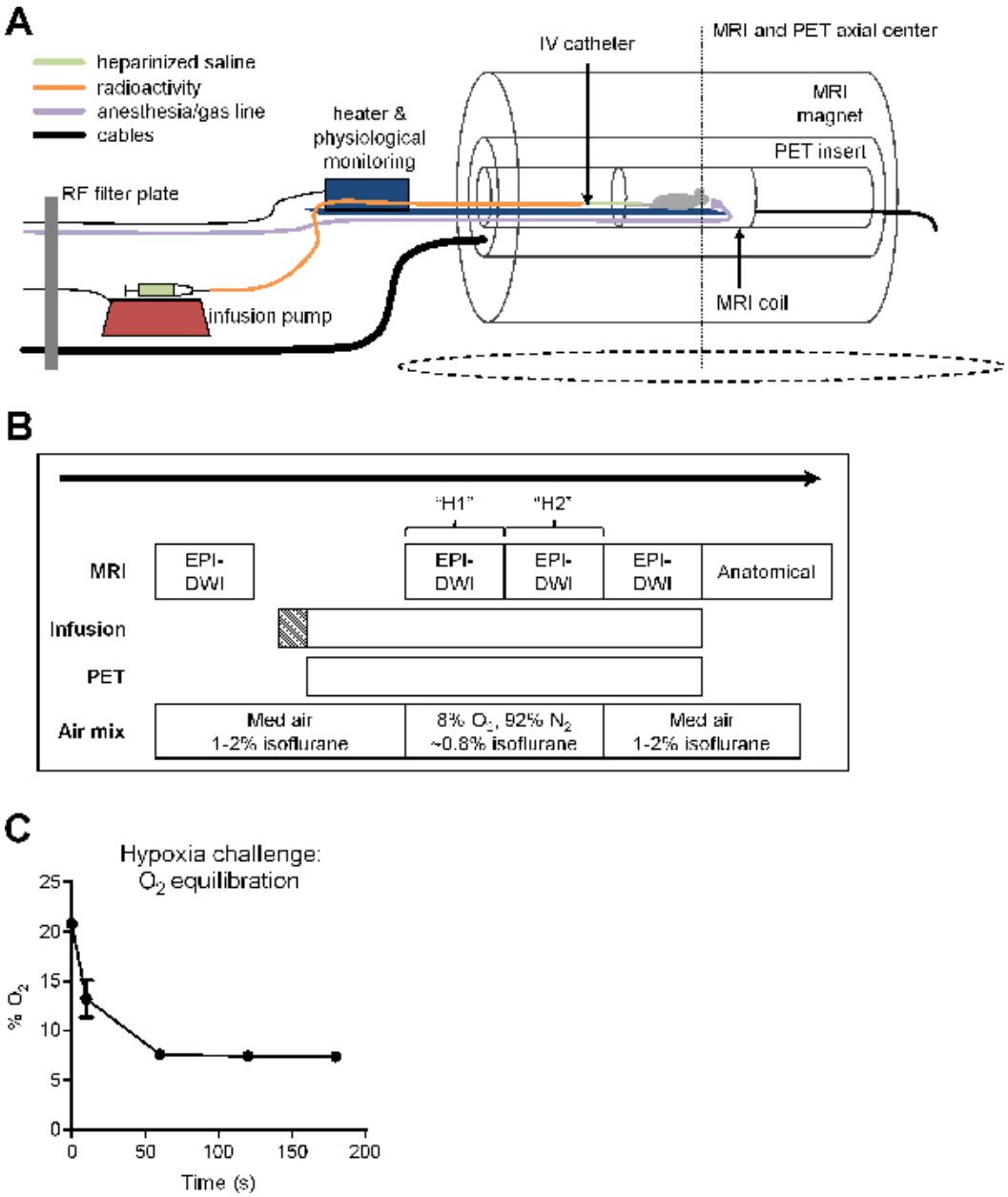

Figure 2. (A) Representative diagram of the physical arrangement of equipment. The PET insert is positioned in the bore of the magnet, and the MRI coil is in turn positioned in the bore of the PET insert. The animal bed, along with physiological monitoring (respiration pad not shown), anesthesia line, and IV catheter runs into the bore as shown. The dotted ring denotes a safety margin for the stray magnetic field – it may be necessary to place equipment with magnetic components outside of this region but within the MRI room (following all safety precautions). **(B)** Diagram summarizing the temporal progression of the experiment. **(C)** Representative results of initial changes in O_2 level delivered to the animal immediately after the start of the hypoxia challenge. Within approximately 1 min, hypoxic conditions can be achieved, as measured by an O_2 meter placed in a 0.5 L induction box (not shown), in-line with the anesthesia system. Please click here to view a larger version of this figure.

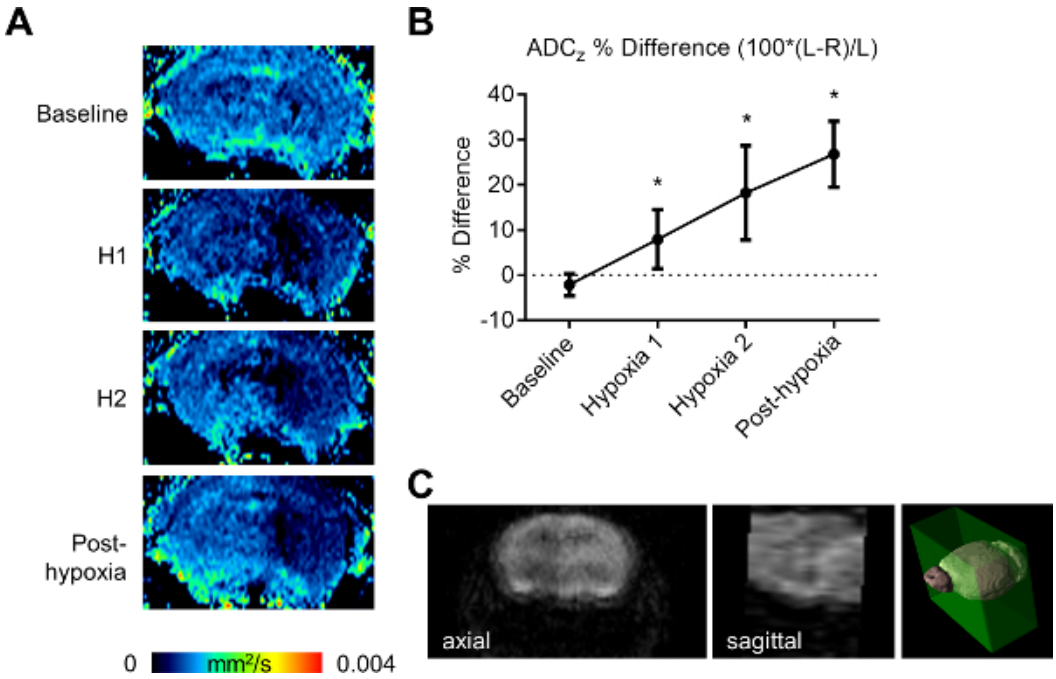

Figure 3. (A) Example of parametric ADC_z maps acquired at baseline and through post-hypoxia. **(B)** Plot showing %L-R difference in ADC_z from baseline to post-hypoxia. Asterisks indicate a significant difference ($p < 0.05$, unpaired *t*-test) compared to baseline value. Error bars represent +/- one standard deviation. **(C)** Example of an EPI-DWI acquisition (axial, sagittal, and 3D views to show extent of the FOV). Please click here to view a larger version of this figure.

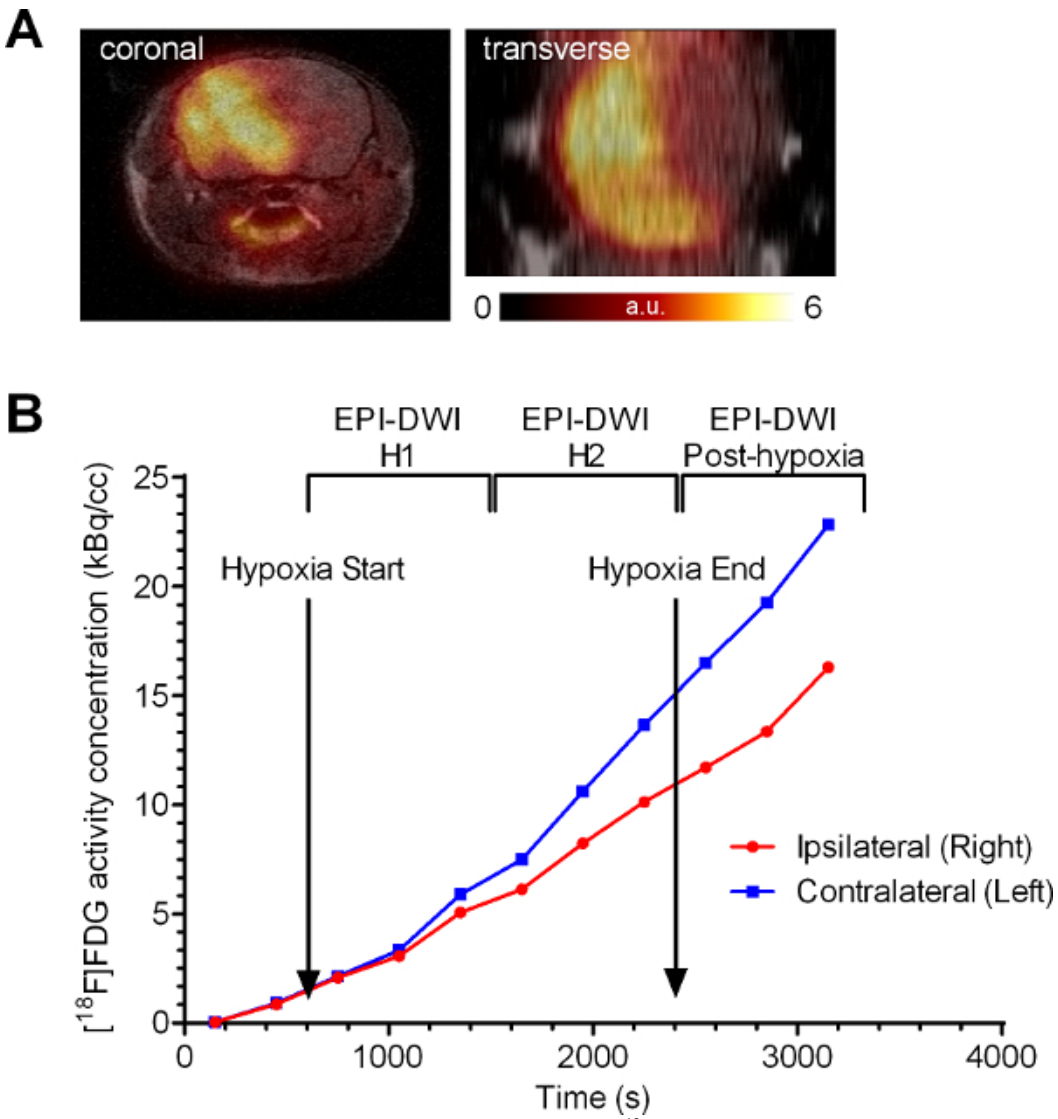

Figure 4. (A) Coronal and transverse slice of an animal showing [^{18}F]FDG uptake. The PET image is in the foreground and is registered and fused with an anatomical MRI image in the background for visualization. The PET data are summed across all frames. **(B)** In the same animal, [^{18}F]FDG time activity curve for the contralateral hemisphere (blue) and ipsilateral hemisphere (red). Please click here to view a larger version of this figure.

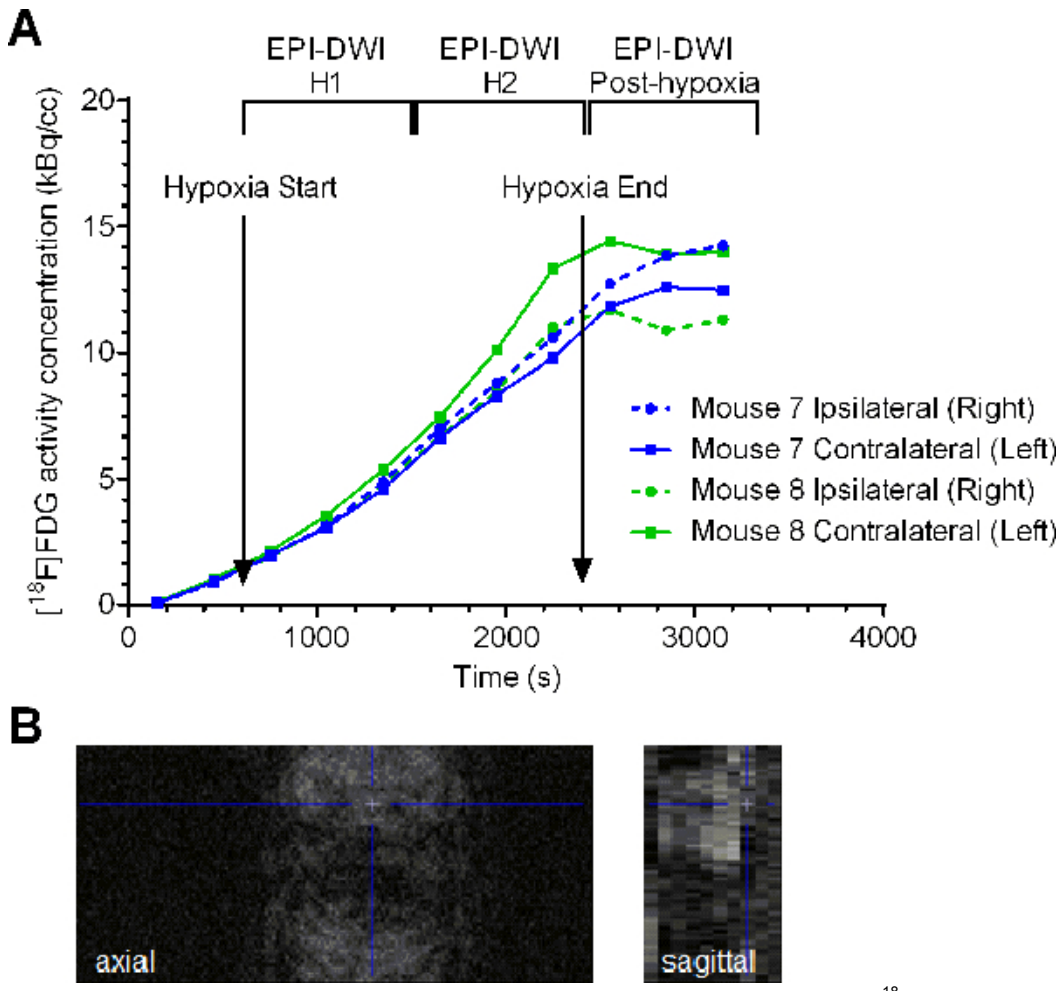

Figure 5. (A) Time activity curves of contralateral (solid) and ipsilateral (dotted) hemisphere [^{18}F]FDG uptake – shown on the same axis are examples of an unexpected [^{18}F]FDG time activity curve (blue) and animal death at the end of H2 (at 45 min, green). **(B)** Ghosting artifacts due to potential hardware-based RF faults. Please click here to view a larger version of this figure.

Imaging Acquistion Parameters and Hardware Acquisition	
Diffusion MRI (EPI-DWI)	
Acqusition time	15 min
Matrix size	256 x 64
Slices	10
FOV	30 x 14 x 8 mm
Voxel size	0.117 x 0.219 x 0.8 mm
Effective spectral bandwidth	150 kHz
TE	41 msec
TR	3,000 msec
Averages	6
k-space segments	16
b-values	0, 400, 800 sec/mm^2
Anatomical MRI (MSME)	
Acquisition time	5 min
Matrix size	256 x 256
Slices	16

FOV	30 x 22 x 12.8 mm
Voxel size	0.117 x 0.086 x 0.8 mm
TE	14 msec
TR	1,000 msec
Averages	1
Repetitions	1
Point-Resolved Spectroscopic Scan (PRESS)	
Acquisition time	15 s
Voxel size	3.9 x 6 x 9 mm
TE	20 msec
TR	2,500 msec
Averages	6
FieldMap	
Acquisition time	1 min 21 sec
1st TE	1.49 msec
2nd TE	5.49 msec
TR	20 msec
Averages	1
PET Acquisition, Histogram, and Reconstruction Parameters	
Tracer	[^{18}F]FDG
Infusion rate	4.44 µL/min
Acquisition time	60 min
Image size per slice	128 x 128
Slices	99
Voxel size	0.4 x 0.4 x 0.6 mm
Dynamic framing	12 x 300 sec
Reconstruction type	OS-MLEM (6 subsets, 6 iterations)

Table 1. MRI pulse sequence parameters for scans described in protocol, and PET acquisition, histogram, and reconstruction parameters.

Discussion

Simultaneous anatomic MRI, and dynamic DWI-MRI and [^{18}F]FDG PET data were successfully acquired from experimental animals during hypoxic challenge following common carotid artery ligation. This represents a powerful experimental paradigm for multimodal imaging of the rapidly evolving pathophysiology associated with ischemic insults in the brain and could readily be extended to study other PET radiotracers (for example markers of neuroinflammation) and MRI sequences, as well as the impact of interventional strategies during or shortly after ischemic challenge.

For successful execution of simultaneous PET/MRI imaging during hypoxic challenge in the cerebral H-I model, logistics must be considered and the methods adjusted accordingly. Factors potentially affecting the temporal arrangement of the experiment include, but are not limited to: 1) source of radioactivity – depending on the radiotracer used, half-life of the radionuclide, and specific activity requirements, this may affect the possible total number of animals imaged; 2) room layout – this may affect the lengths of tubing used and thus the injected dose, or may require additional steps to maintain injected dose. This may also have a small effect on the time to reach equilibrium for gas mixtures in the anesthesia tubing; 3) animal weight – some institutions may impose a limit on the total injected volume for survival procedures (*e.g.*, less than 1% of body weight), in turn potentially affecting tubing length and infusion pump rate settings; 4) tracer delivery – a bolus, infusion, or bolus plus infusion delivery may be used, as determined by radiotracer pharmacokinetics and expected observable changes – the latter two are especially useful to follow dynamic changes [24].

Design of the PET and MRI image acquisition protocols, particularly given the limited time with which to work, is another crucial factor in this experiment. If using an echo-planar imaging (EPI)-based DWI sequence (EPI-DWI) as presented here, important considerations include

scan duration, field of view, and diffusion gradient weighting and directions. While adjusting these parameters, inherent issues with EPI-DWI must also be addressed, including ghosting, signal dropout, and gradient duty cycle limitations. The use of respiratory gating may be used to address issues due to motion. **Table 1** describes the MRI acquisition parameters used along with information on the PET hardware, acquisition parameters, and tracer delivery parameters. For quantification of PET data, detector normalization must be applied. Though not done in our case, further steps can be taken to achieve more accurate quantification, including attenuation correction using segmented MRI data and scatter correction. The former may not be necessary in small animals as the degree of attenuation is small and can be accounted for using similar-sized calibration objects. Depending on the MRI sequence used, it may also be necessary to consider any significant BOLD effects on T2* [25]. In addition, the effect of anesthetic and carrier gas on blood glucose may need to be considered when using [^{18}F]FDG [26].

Checks should be carried out to ensure there is no significant mutual interference between the PET and MRI systems, or between the imaging systems and other instrumentation used in the experiment. In our experience, there was no significant difference in the PET or MRI image quality when acquired individually or simultaneously, although we have observed momentary loss in counts in the PET system due to spurious signals in the PSAPD-based detectors induced by rapid gradient switching, an effect that has been noted by others [12]. Another issue observed was RF noise from the infusion pump power supply disturbing PET detector acquisition resulting in loss of data. This was resolved by replacing the original AC adaptor with a laboratory-quality power supply. More PET/MRI hardware configurations are described in the literature, and adjustments to this protocol may be required to accommodate unique setups [12,27].

The imaging workflow may be modified in order to optimize conditions for different MRI pulse sequences or PET tracers and acquisition schemes. For instance, severity of injury in the cerebral H-I model has been shown to be modulated by, among other conditions, the duration of hypoxia [11]. Increasing the length of the hypoxic challenge may allow acquisition of DWI data at finer temporal resolution, or allow for more robust hemispherical uptake comparisons for PET tracers. Other aspects of the protocol may be adjusted based on available resources and personnel. For instance, surgeries may be staggered and run parallel to imaging sessions in order to reduce the variability in the time between CCA ligation and hypoxia.

In this protocol, simultaneous PET and MRI acquisition, in addition to the physiological challenge, imposes mutual limits on one another in terms of timing. In optimizing the EPI-DWI sequence, it was found that having additional diffusion directions while maintaining image quality would increase acquisition time beyond acceptable limits for performing multiple acquisitions during the hypoxic challenge. Thus, diffusion gradients were applied solely along the z-axis. In addition, the adaptation of animal models to an imaging protocol may require some modification – in our case the standard cerebral hypoxia-ischemia model was altered by the injection of additional fluid (0.2 ml of the radiotracer) during the hypoxic challenge.

Given the complexity of timing in this experiment, there are many failure modes at different steps along the way that may delay the experiment at best, or end the experiment without salvageable data in the worst case. Consistency at each step, from animal model generation to imaging, is crucial and may only be achieved by preparation and practice. Mastery of the techniques presented in this paper will allow for the robust application of simultaneous PET/MRI imaging to a variety of animal models and PET and MRI contrast methods.

Disclosures

JM and SW are employees of Genentech.

Acknowledgements

The authors would like to acknowledge the Center for Molecular and Genomic Imaging at UC Davis and the Biomedical Imaging Department at Genentech. This work was supported by a National Institutes of Health Bioengineering Research Partnership grant number R01 EB00993.

References

1. Donnan, G. A., *et al.* Stroke. *The Lancet.* **371**, 1614-1623 (2008).
2. Turner, R. C., *et al.* The science of cerebral ischemia and the quest for neuroprotection: navigating past failure to future success: A review. *Journal of Neurosurgery.* **118**, 1072-1085 (2013).
3. Vannucci, R. C., Perlman, J. M. Interventions for perinatal hypoxic-ischemic encephalopathy. *Pediatrics.* **100**, 1004-1014 (1997).
4. Chicha, L., *et al.* Stem cells for brain repair in neonatal hypoxia–ischemia. *Child's Nervous System.* **30**, 37-46 (2014).
5. Barks, J. D. Current controversies in hypothermic neuroprotection. *Seminars in Fetal and Neonatal Medicine.* **13**, (1), 30-34 (2008).
6. Jantzie, L. L., *et al.* Neonatal ischemic stroke: a hypoxic-ischemic injury to the developing brain. *Future Neurology.* **3**, 99-102 (2008).
7. James, A., Patel, V. Hypoxic ischaemic encephalopathy. *Paediatrics and Child Health.* **24**, (9), (2014).
8. Levine, S. Anoxic-ischemic encephalopathy in rats. *The American Journal of Pathology.* **36**, (1), (1960).
9. Vannucci, S. J., *et al.* Experimental stroke in the female diabetic, db/db, mouse. *Journal of Cerebral Blood Flow & Metabolism.* **21**, 52-60 (2001).
10. Sheldon, R., *et al.* Strain-related brain injury in neonatal mice subjected to hypoxia-ischemia. *Brain Research.* **810**, 114-122 (1998).
11. Adhami, F., *et al.* Cerebral ischemia-hypoxia induces intravascular coagulation and autophagy. *American Journal of Pathology.* **169**, (2), 566-583 (2006).
12. Catana, C., *et al.* Simultaneous in vivo positron emission tomography and magnetic resonance imaging. *Proceedings of the National Academy of Sciences.* **105**, 3705-3710 (2008).

13. Judenhofer, M. S., *et al.* Simultaneous PET-MRI: a new approach for functional and morphological imaging. *Nature Medicine*. **14**, 459-465 (2008).
14. Wehrl, H. F., *et al.* Simultaneous PET-MRI reveals brain function in activated and resting state on metabolic, hemodynamic and multiple temporal scales. *Nature Medicine.* **19**, 1184-1189 (2013).
15. Judenhofer, M. S., Cherry, S. R. Applications for preclinical PET/MRI. *Seminars in Nuclear Medicine*. **43**, (1), 19-29 (2013).
16. Wehrl, H. F., *et al.* Preclinical and Translational PET/MR Imaging. *Journal of Nuclear Medicine.* **55**, Suppl 2. 11S-18S (2014).
17. Heiland, S. Diffusion and Perfusion Weighted MR Imaging in Acute Stroke: Principles, Methods, and Applications. *Imaging Decisions MRI*. **7**, 4-12 (2003).
18. Loubinoux, I., *et al.* Spreading of vasogenic edema and cytotoxic edema assessed by quantitative diffusion and T2 magnetic resonance imaging. *Stroke.* **28**, 419-427 (1997).
19. Ouyang, Y., *et al.* Evaluation of 2-[18F]fluoroacetate kinetics in rodent models of cerebral hypoxia–ischemia. *Journal of Cerebral Blood Flow & Metabolism.* **34**, (5), 836-844 (2014).
20. Kuhl, D. E., *et al.* Effects of stroke on local cerebral metabolism and perfusion: mapping by emission computed tomography of 18FDG and 13NH3. *Annals of Neurology.* **8**, 47-60 (1980).
21. Planas, A. M. Noninvasive Brain Imaging in Small Animal Stroke Models: MRI and PET. *Neuromethods.* **47**, 139-165 (2010).
22. Marik, J., *et al.* PET of glial metabolism using 2-18F-fluoroacetate. *Journal of Nuclear Medicine.* **50**, (6), 982-990 (2009).
23. Martín, A., *et al.* Depressed glucose consumption at reperfusion following brain ischemia does not correlate with mitochondrial dysfunction and development of infarction: an in vivo positron emission tomography study. *Current Neurovascular Research.* **6**, 82-88 (2009).
24. Carson, R. E. PET physiological measurements using constant infusion. *Nuclear Medicine and Biology.* **27**, 657-660 (2000).
25. Greve, J. M. The BOLD effect. *Methods in Molecular Biology.* **771**, 153-169 (2011).
26. Flores, J. E., *et al.* The effects of anesthetic agent and carrier gas on blood glucose and tissue uptake in mice undergoing dynamic FDG-PET imaging: sevoflurane and isoflurane compared in air and in oxygen. *Molecular Imaging and Biology.* **10**, 192-200 (2008).
27. Delso, G., Ziegler, S. PET/MRI system design. *European Journal of Nuclear Medicine and Molecular Imaging.* **36**, 86-92 (2009).

